Electronic Supplementary Material (ESI) for Journal of Analytical Atomic Spectrometry.
This journal is © The Royal Society of Chemistry 2021

Supplementary Information

LA-ICP-MS using a nitrogen plasma source

Christoph Neff, Pascal Becker, Bodo Hattendorf*, Detlef Günther*

Laboratory of Inorganic Chemistry, Department of Chemistry and Applied Biosciences, ETH Zurich, Vladimir-Prelog-Weg 1, 8093 Zürich, Switzerland

*corresponding authors: detlef.guenther@sl.ethz.ch, bodo@inorg.chem.ethz.ch

LA-(Ar-ICP)-MS experiments were performed using an Agilent 7500cs (Agilent, USA). NIST SRM 612 was quantified using NIST SRM 610 as external standard and $^{44}Ca^{+}$ was used as internal standard. For each LA-(Ar-ICP)-MS measurement, 30 s of gas blank were acquired followed by 50 s of ablation. LA-(Ar-ICP)-MS operating conditions were applied according to **Table S1**.

Table S1 LA-(Ar-ICP)-MS operating conditions.

Laser fluence	15-20 J/cm^2
Laser repetition rate	10 Hz
Laser spot diameter	60 µm
Ablation mode	Hole-drilling (bulk analysis)
Ablation gas flow (He)	0.95 L/min
Carrier gas flow (Ar)	0.65 L/min
Auxiliary gas flow (Ar)	0.92 L/min
Cooling gas flow (Ar)	15.2 L/min
Plasma power	1400 W
Sampler cone	1.0 mm Ø, Pt
Skimmer cone	0.3 mm Ø, Pt

Unknown gas blank species. Four unknown species were detected in the dry (N_2-ICP)-MS gas blank at m/z 80, 82, 108, 110. The mass difference of 28 indicated that the species at 108 and 110 m/z are likely caused by $^{14}N_2$ adducts from the species at 80 and 82 m/z. Similar intensity ratios for of [80]/[82] (2.4) and [108]/[110] (2.2) suggest a similar reactivity with N_2. Therefore, the origin of the species at 80 and 82 m/z was further investigated. These signals cannot be explained by the species $^{80}Kr^{+}/^{82}Kr^{+}$ or $^{80}Se^{+}/^{82}Se^{+}$, as they did not fit the isotopic abundance of these elements. Oxides, nitrides and doubly charged ions such as $^{64}Zn^{16}O^{+}/^{66}Zn^{16}O^{+}$, $^{66}Zn^{14}N^{+}/^{68}Zn^{14}N^{+}$, $^{66}Zn^{14}N^{+}/^{66}Zn^{16}O^{+}$, $^{160}Gd^{2+}$, $^{160}Dy^{2+}$, $^{164}Dy^{2+}$, or $^{164}Er^{2+}$ were also excluded, as they did not match with the isotopic abundance of these elements and as Zn^{+}, Gd^{+}, Dy^{+}, and Er^{+} were not detected in the gas blank. Other polyatomic species such as $^{79}Br^{1}H^{+}/^{81}Br^{1}H^{+}$ or $^{12}C^{16}O_2{}^{35}Cl^{1}H^{+}/^{12}C^{16}O_2{}^{37}Cl^{1}H^{+}$ ($HCl+CO_2$) were also excluded as Br^{+} and Cl^{+} were not detected in the gas blank. The combinations of $^{40}Ar_2{}^{+}/^{40}Ar^{14}N_3{}^{+}$, $^{12}C_2{}^{14}N_4{}^{+}/^{12}C^{14}N_5{}^{+}$, and

$^{63}Cu^{16}O^{1}H^{+}$/$^{65}Cu^{16}O^{1}H^{+}$ were examined by ablating pure copper (> 99.9%), graphite (pencil lead, Farber-Castell, Germany), and by adding 0.1 L/min Ar gas (99.996%, PanGas AG, Switzerland) to the dry (N_2-ICP)-MS gas blank (**Figure S1b-d**). The intensities of the signals at 80 and 82 m/z did not change, indicating that Ar, C, and Cu were not part of these species. Therefore, an assignment of the species at 80, 82, 108, 110 m/z cannot be given.

In addition, these experiments revealed the formation of other cluster species. The ablation of copper formed $^{63}Cu^{14}N_2^{+}$ and $^{65}Cu^{14}N_2^{+}$ clusters and to a lower extent $^{63}Cu^{14}N^{+}$ and $^{65}Cu^{14}N^{+}$. The ablation of graphite intensified the signals for 40 and 44 m/z indicating the formation of $^{12}C^{14}N_2^{+}$, $^{12}C^{16}O_2^{+}$, $^{14}N_2{}^{16}O^{+}$ and/or residues of Ca in the graphite pencil lead. Adding 0.1 L/min of Ar to the carrier gas intensified the $^{36,38,40}Ar^{+}$ signals and also $^{40}Ar^{14}N^{+}$ and $^{40}Ar^{14}N_2^{+}$.

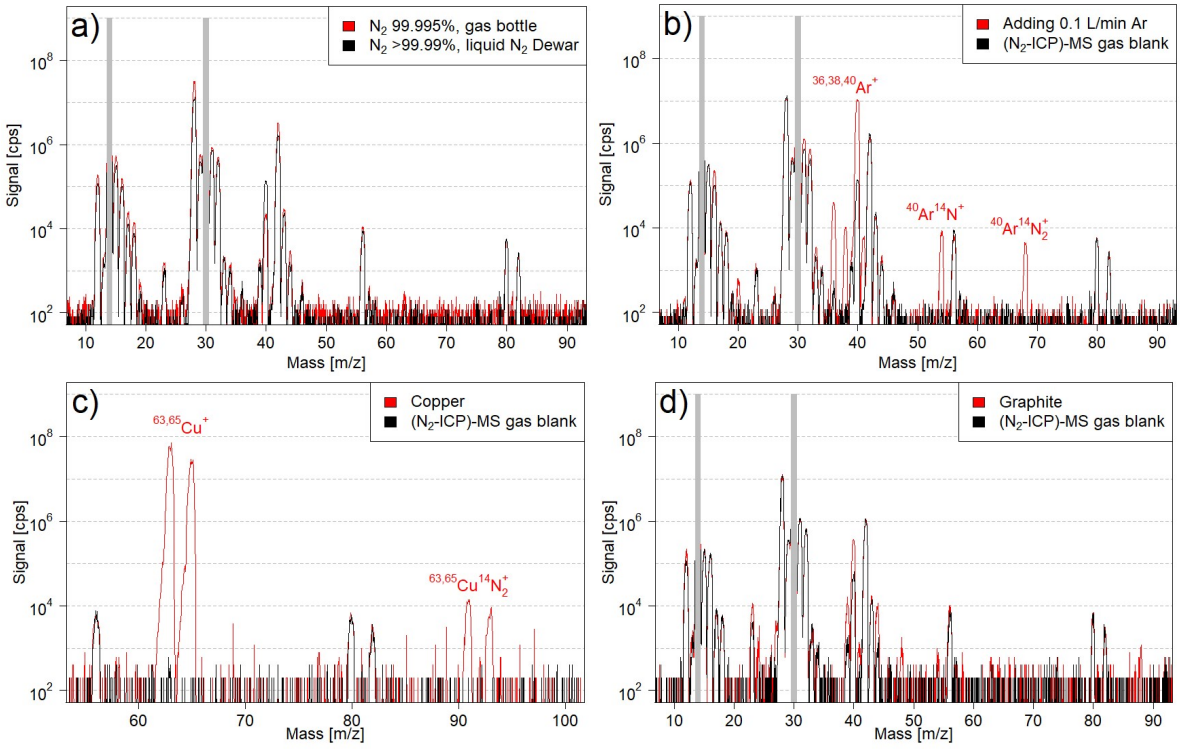

Figure S1 a) N_2 from a 50 L gas bottle (99.995%), b) adding 0.1 L/min Ar, c) ablation of copper, and d) ablation of graphite compared to the gas blank spectrum of (N_2-ICP)-MS using N_2 from a liquid N_2 Dewar (> 99.99%).

Table S2 NIST SRM 610 analyzed with LA-(N_2-ICP)-MS. Figures of merit for selected isotopes of Ca, Cr, Fe, Se, and Te.

Isotope	Bg corr signal [cps]	Background [cps]	Sensitivity [cps/(mg/kg)]	LOD [mg/kg]
^{40}Ca	52'000'000	56'000	600	3
^{42}Ca	110'000	1'170'000	1.4	13000
^{43}Ca	64'000	12'100	0.8	500
^{44}Ca	1'010'000	450	12	6
^{52}Cr	147'000	6	400	0.02
^{53}Cr	17'600	3	40	0.2
^{56}Fe	181'000	6'500	400	0.8
^{57}Fe	4'200	90	9	3
^{77}Se	900	7	6	1
^{78}Se	2'400	2	17	0.3
^{80}Se	5'300	5'300	40	6
^{82}Se	1'100	2'200	8	22
^{125}Te	5'500	1	18	0.2
^{126}Te	14'600	2	50	0.1
^{128}Te	25'000	4	80	0.09

Table S3 Figures of merit for 64 elements in NIST SRM 610 analyzed with LA-(N_2-ICP)-MS. For isotopes where an average background signal of 0 cps was measured one data point with 100 cps (1 count, 10 ms dwell time) was added to calculate the LOD according to Longerich et al.[1] These LODs were marked with an asterisk and were in good agreement with other LA-(N_2-ICP)-MS measurements of NIST SRM 610.

Isotope	Bg corr signal [cps]	Background [cps]	Sensitivity [cps/(mg/kg)]	LOD [mg/kg]
^{7}Li	40'000	50	80	0.4
^{9}Be	18'000	3	40	0.2
^{11}B	21'000	10	60	0.2
^{23}Na	25'000'000	1'000	250	0.6
^{25}Mg	9'000	0	20	0.2*
^{27}Al	1'900'000	70	180	0.2
^{29}Si	1'400'000	196'000	4	1'000
^{39}K	300'000	18'700	700	0.9
^{40}Ca	56'000'000	77'000	700	6
^{45}Sc	240'000	6	500	0.02
^{49}Ti	13'000	0	30	0.2*
^{51}V	210'000	5	500	0.02
^{52}Cr	150'000	3	400	0.02
^{55}Mn	240'000	4	500	0.02
^{56}Fe	190'000	7'400	400	1
^{59}Co	110'000	3	300	0.04
^{60}Ni	30'000	3	60	0.1
^{63}Cu	59'000	50	130	0.3
^{66}Zn	22'000	1	50	0.1
^{69}Ga	157'000	5	400	0.02
^{72}Ge	41'000	30	90	0.2
^{75}As	28'000	30	90	0.3
^{78}Se	2'400	1	17	0.2
^{85}Rb	300'000	30	700	0.03
^{88}Sr	460'000	5	900	0.009
^{89}Y	490'000	3	1'100	0.006
^{90}Zr	220'000	3	500	0.01
^{93}Nb	420'000	8	900	0.01
^{95}Mo	56'000	3	140	0.06
^{103}Rh	900	3	700	0.01
^{105}Pd	200	3	190	0.04
^{107}Ag	72'000	4	300	0.03

^{111}Cd	15’000	3	60	0.1
^{115}In	390’000	20	900	0.02
^{118}Sn	80’000	1’000	190	0.7
^{121}Sb	89’000	10	230	0.05
^{128}Te	24’000	5	80	0.1
^{133}Cs	270’000	9	700	0.02
^{137}Ba	43’000	2	90	0.05
^{139}La	330’000	2	700	0.006
^{140}Ce	320’000	3	700	0.008
^{141}Pr	430’000	0	1’000	0.003*
^{146}Nd	73’000	1	170	0.02
^{147}Sm	61’000	1	130	0.03
^{153}Eu	240’000	0	500	0.006*
^{157}Gd	76’000	1	170	0.02
^{159}Tb	550’000	3	1’300	0.005
^{163}Dy	141’000	2	300	0.01
^{165}Ho	610’000	1	1’400	0.002
^{166}Er	205’000	2	400	0.01
^{169}Tm	640’000	2	1’500	0.003
^{172}Yb	144’000	0	300	0.01*
^{175}Lu	640’000	1	1’500	0.002
^{180}Hf	240’000	1	600	0.005
^{181}Ta	620’000	1	1’400	0.002
^{182}W	135’000	1	300	0.01
^{185}Re	25’000	1	500	0.006
^{195}Pt	800	0	250	0.01*
^{197}Au	3’800	0	160	0.02*
^{205}Tl	49’000	3	800	0.007
^{208}Pb	197’000	1	500	0.009
^{209}Bi	280’000	3	700	0.008
^{232}Th	420’000	1	900	0.004
^{238}U	430’000	0	900	0.003*

Table S4 Quantification of selected elements in NIST SRM 612 using LA-(N_2-ICP)-MS and LA-(Ar-ICP)-MS. The confidence intervals were calculated based on four consecutive measurements with a confidence level of 95%. The reference values were based on Jochum et al.[2]

Isotope	Quantified mass fractions with LA-(N_2-ICP)-MS [mg/kg]	Quantified mass fractions with LA-(Ar-ICP)-MS [mg/kg]	NIST SRM 612 ref. values [mg/kg]
^{7}Li	40.5 ± 1.0	40.5 ± 0.4	40.2 ± 1.3
^{9}Be	40.1 ± 1.1	40.4 ± 1.5	37.5 ± 1.5
^{11}B	35.7 ± 1.0	34.9 ± 1.7	34.3 ± 1.7
^{23}Na	104400 ± 900	102100 ± 400	101600 ± 2200
^{25}Mg	56.3 ± 1.7	54.7 ± 1.2	68 ± 5
^{27}Al	10740 ± 210	10750 ± 90	10740 ± 210
^{29}Si	343000 ± 9000	336000 ± 5000	337000 ± 3000
^{39}K	62.2 ± 0.8	59.3 ± 2.1	62.3 ± 2.4
^{52}Cr	35.92 ± 0.06	-	36.4 ± 1.5
^{53}Cr	-	35.8 ± 1.3	36.4 ± 1.5
^{55}Mn	38.6 ± 0.9	38.2 ± 0.3	38.7 ± 0.9
^{56}Fe	46.3 ± 1.2	47.1 ± 0.4	51.0 ± 2.0
^{59}Co	34.9 ± 0.3	34.94 ± 0.14	35.5 ± 1.0
^{66}Zn	37.8 ± 1.8	36.3 ± 1.6	39.1 ± 1.7
^{75}As	33.9 ± 1.3	33.0 ± 0.9	36 ± 6
^{77}Se	-	19 ± 5	16.3 ± 1.9
^{78}Se	18.8 ± 1.8	-	16.3 ± 1.9
^{85}Rb	31.5 ± 0.4	31.5 ± 0.4	31.4 ± 0.4
^{107}Ag	22.4 ± 0.9	21.4 ± 0.6	22.0 ± 0.3
^{115}In	37.0 ± 0.7	36.88 ± 0.17	38.9 ± 2.1
^{125}Te	34.4 ± 1.0	34.4 ± 1.3	30.9
^{128}Te	35.4 ± 1.3	33.8 ± 0.5	30.9
^{133}Cs	42.1 ± 0.8	41.35 ± 0.17	42.7 ± 1.8
^{159}Tb	36.3 ± 0.7	37.0 ± 0.6	37.6 ± 1.1
^{208}Pb	38.6 ± 0.4	37.4 ± 1.2	38.57 ± 0.20
^{232}Th	36.9 ± 0.4	37.7 ± 0.6	37.79 ± 0.08
^{238}U	37.3 ± 0.7	37.3 ± 0.4	37.38 ± 0.08

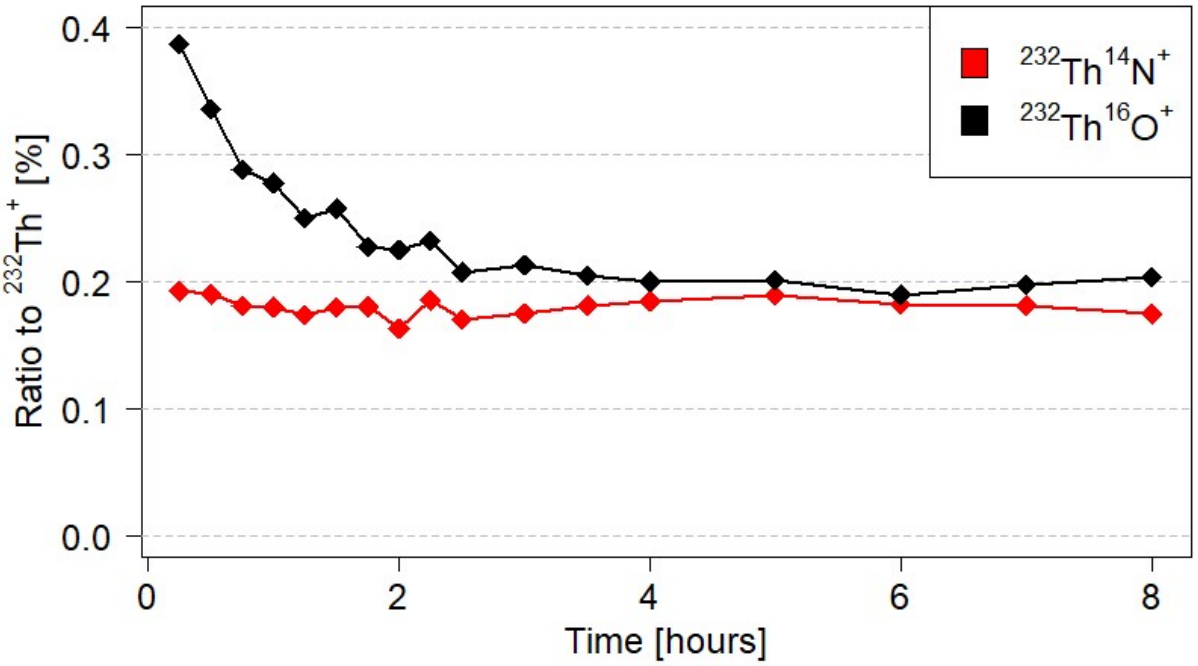

Figure S2 $^{232}Th^{14}N^+/^{232}Th^+$ and $^{232}Th^{16}O^+/^{232}Th^+$ ratios measured in the LA-(N_2-ICP)-MS long-term study.

References

1. H. P. Longerich, S. E. Jackson and D. Gunther, *Journal of Analytical Atomic Spectrometry*, 1996, **11**, 899-904.
2. K. P. Jochum, U. Weis, B. Stoll, D. Kuzmin, Q. Yang, I. Raczek, D. E. Jacob, A. Stracke, K. Birbaum, D. A. Frick, D. Günther and J. Enzweiler, *Geostandards and Geoanalytical Research*, 2011, **35**, 397-429.